Journal of Electrical Engineering, Vol. 76, No. 6, 2025, pp. 546-556
https://reference-global.com/journal/JEE

Advanced control of five-phase PMSM using combined fractional-order super-twisting algorithm with modified SVM approach

Fayçal Mehedi[1*], Abdelkader Yousfi[2], Ismail Bouyakoub[1], Zakaria Reguieg[1]

Multi-phase machine drives are gaining attention in the fields of electrical machines and control due to their benefits. However, the application of these motors is challenging due to the inefficiency of conventional control techniques in multiphase systems. This paper presents an enhanced direct torque control (DTC) method for a five-phase permanent magnet synchronous motor (PMSM). The problems of variable switching frequency and limitations of the proportional integral (PI) controller have been overcome by integrating a fractional-order super-twisting sliding mode algorithm (FOSTSMA) with a modified space vector modulation (MSVM) technique. This MSVM approach determines minimum and maximum voltage values to achieve superior performance. The proposed DTC-MSVM-FOSTSMA strategy significantly outperforms traditional DTC by offering better robustness and an improved dynamic response. Simulation results in MATLAB confirmed the proposed DTC-MSVM-FOSTSMA strategy's efficacy in enhancing motor performance. Compared to conventional DTC and DTC-MSVM-PI methods, this approach yielded substantial improvements: an 83.33% and 78.57% reduction in response time, a 61.84% and 32.55% decrease in torque ripple, and a 58.64% and 34.52% minimization of stator flux ripples, respectively. Additionally, the proposed control exhibits robust performance under parameter variations.

Keywords: direct torque control, fractional-order control, five-phase PMSM, super-twisting algorithm, SVM approach

1 Introduction

Multi-phase machine (MPM) drive systems are now being integrated into more applications. As a result, these systems must be able to handle a variety of operating conditions, especially in applications that require high reliability and robustness against internal and external disturbances. The benefits of MPM systems over traditional three-phase designs are significant, encompassing improved performance and robustness, less per-phase current, lower torque fluctuations, a greater power output capacity, and a steadier speed response [1-3]. MPMs are becoming increasingly popular in applications that require high reliability, such as pump drives, robotics, energy conversion systems, electric vehicles, and marine propulsion [4, 5].

The permanent magnet synchronous motor (PMSM) is increasingly favored in high-performance applications due to its superior power density, efficiency, and torque capabilities [6, 7]. Among the various control techniques developed for PMSM drives, field-oriented control (FOC) and direct torque control (DTC) are prominent [8, 9]. DTC is often regarded as more suitable for PMSMs than FOC because of its faster torque dynamics. Despite this advantage, conventional DTC is plagued by issues like high torque, flux, and current ripples, variable switching frequency, and poor performance at low speeds [10]. Consequently, numerous strategies have been introduced to address these limitations [11, 12]. In [13], the authors developed a sensorless DTC approach for a five-phase PMSM using a 7-level hysteresis torque controller. A model-based predictive control approach was integrated into the DTC framework in [14], targeting loss reduction and improved reliability for a five-phase PMSM drive system. To combat variable switching frequency, DTC based space vector modulation (SVM) was proposed to enforce constant switching frequency [13, 14]. Elsewhere, multilevel inverters were integrated to improve control quality [15], though this escalated switching losses. A separate avenue of research utilized intelligent optimization techniques like genetic algorithms (GA) and particle swarm optimization (PSO) to auto-tune proportional-integral (PI) gains, which improved transient performance but failed to substantially curb steady-state ripple [16, 17]. In response to these limitations, recent studies are increasingly pioneering data-driven and artificial intelligence (AI) based methods, such as artificial neural networks (ANN) and fuzzy inference systems, to intelligently augment DTC performance [18, 19]. In [20], the authors introduced a cascaded ANN to enhance the model predictive DTC for a PMSM inverter. This

[1] Laboratoire Génie Electrique et Energies Renouvelables (LGEER), Faculty of Technology, Hassiba Benbouali University of Chlef, Chlef 02000, Algeria
[2] Laboratory LAGC, Faculty of Science and Technology, Djilali Bounaama University of Khemis Miliana, Khemis Miliana, Algeria
*Corresponding author: f.mehedi@univ-chlef.dz

https://doi.org/10.2478/jee-2025-0057, Print (till 2015) ISSN 1335-3632, On-line ISSN 1339-309X

intelligent framework allows for the real-time adjustment of weighting factors in response to operational changes, thereby refining their optimization. Experimental validation confirmed that this method boosts the inverter's overall performance.

A systematic classification of the diverse control schemes employed in PMSMs is illustrated in Fig. 1. This flowchart offers a structural classification of PMSM control strategies, organizing them into the primary groups of classical, linear, nonlinear, and advanced intelligent techniques.

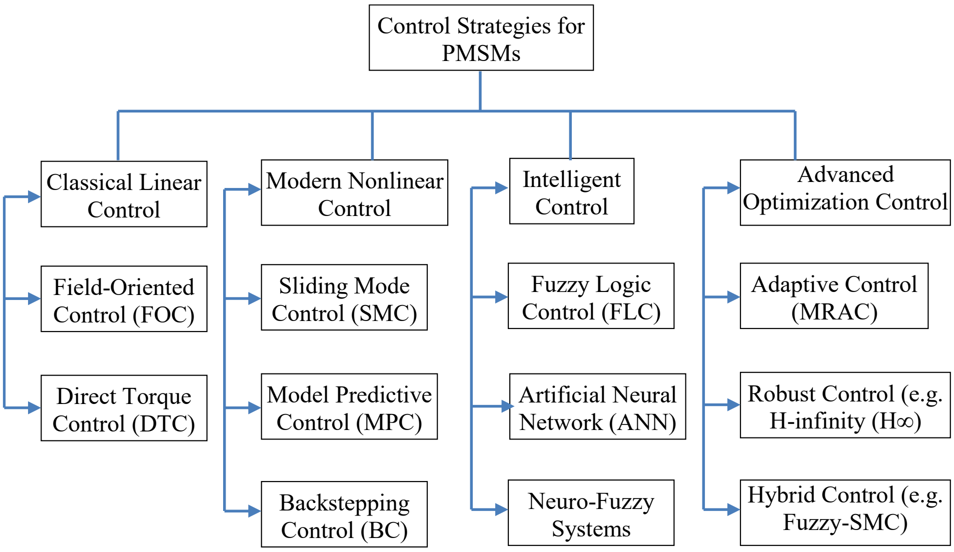

Fig. 1. Flowchart classifying different control strategies for PMSM

Sliding mode control (SMC) has become an increasingly popular control strategy because it is simple to implement, robust against external disturbances, and largely insensitive to variations in system parameters [21]. However, the chattering phenomenon, a recognized shortcoming of traditional SMC, has been widely investigated by researchers [21, 22]. It generates oscillations in torque and current, which in turn result in detrimental mechanical vibration.

To mitigate the chattering phenomenon associated with conventional SMC, higher-order SMC (HOSMC) offers a viable solution. As an advanced variant of SMC, HOSMC introduces the discontinuous control action to the higher derivatives of the sliding variable instead of applying it directly to the sliding surface, thereby significantly reducing chattering. Second-order SMC (SOSMC) algorithms are widely adopted in practical applications as effective substitutes for traditional SMC [23]. In [24], a SOSMC strategy was implemented to enhance the control performance of a 5-phase induction motor via a robust nonlinear control law, which effectively compensates for system uncertainties without sacrificing structural simplicity.

The conventional SVM technique offers advantages like lower current total harmonic distortion (THD) and an 80% increase in output voltage over PWM. However, its deployment is challenging due to complex control schemes based on sector and angle computation [25]. In [26], the authors presented details a simplified SVM method effective for three-phase inverter control. This technique establishes switching actions by calculating the min and max values of the three-phase voltages.

The application of fractional-order calculus offers significant advantages for improving system characterristics and overcoming inherent flaws in conventional control methods. This strategy is regarded as a robust mathematical solution for controlling electrical systems due to its efficiency and simplicity as a nonlinear approach, which proves especially valuable in maintaining performance during machine failures [27]. In [28], the fractional-order SMC (FOSMC) strategy serves as a viable alternative for achieving enhanced regulatory performance in complex or turbulent systems. This approach provides greater flexibility via its incorporation of additional tuning parameters. Consequently, it exhibits superior disturbance rejection, resulting in improved adaptability, stability, and overall control efficacy, particularly under demanding operational conditions.

This research utilizes a novel framework that formulates its control law by synergistically combining the principles of fractional-order calculus with a super-twisting sliding mode algorithm (FOSTSMA). The proposed approach is designed to develop advanced controllers that supersede conventional PI regulators in the flux, torque, and speed control loops of a DTC architecture of five-phase PMSMs. This methodology combines a robust nonlinear FOSTSMA with a modified space vector modulation (MSVM) technique. The MSVM technique, which determines the minimum and maximum values of the five-phase voltages, enhances overall performance. A key advantage of the integrated FOSTSMA-DTC-MSVM strategy is its enhancement of system stability and smoother control performance. This is achieved by mitigating chattering phenomena through the application of fractional-order calculus and higher-order sliding modes. Furthermore, a primary benefit of this approach over traditional methods is its ability to concurrently deliver robust performance, achieve rapid settling times, and minimize overshoot.

This paper is organized in the following manner: The DTC modeling of the five-phase PMSM is presented in Section 2. Section 3 outlines the suggested five-phase MSVM technique. The novel control scheme, which combines a FOSTSMA-DTC and MSVM technique, is introduced in Section 4. Section 5 provides simulation results under various operating conditions, including reference tracking, disturbance rejection, and parameter variation scenarios. This section also features a comparative analysis of the conventional DTC, the DTC-MSVM-PI method, and the proposed DTC-MSVM-FOSTSMA approach. A summary of the conclusions drawn from this work is provided in Section 6.

2 Mathematical modelling

2.1 The five-phase PMSM model

The stator voltage of a five-phase PMSM can be expressed in the d-q and x-y subspace by the following equation [29]:

$$\begin{cases} v_{ds} = R_s i_{ds} + \dfrac{d}{dt}\left(L_d i_{ds} + \varphi_f\right) - \omega_r L_q i_{qs} \\ v_{qs} = R_s i_{qs} + \dfrac{d}{dt} L_q i_{qs} + \omega_r\left(L_d i_{ds} + \varphi_f\right) \\ v_{xs} = R_s i_{xs} + \dfrac{d}{dt} L_{ls} i_{xs} \\ v_{ys} = R_s i_{ys} + \dfrac{d}{dt} L_{ls} i_{ys} \end{cases} \tag{1}$$

where v_{ds}, v_{qs}, v_{xs}, v_{ys}, i_{ds}, i_{qs}, i_{xs}, i_{ys} are the components of stator voltages, currents in *d*-*q*, *x*-*y* subspaces, respecttively, L_d, L_q are the stator inductances in the *d*-*q* subspaces, ϕ_f is magnetic flux, ω_r is the rotation speed, L_{ls} is the leakage inductances, R_s is the stator resistance.

The electromagnetic torque T_e is

$$T_e = \frac{5}{2} p\left(\left(L_d - L_q\right) i_{ds} i_{qs} + \varphi_f i_{qs}\right) \tag{2}$$

The mechanical dynamics of the motor is expressed as

$$J_m \frac{d\omega_r}{dt} = pT_e - pT_l - f_m \omega_r \tag{3}$$

where, T_l is the load torque, f_m is the viscous damping, P is the number of pole pairs, J_m is the inertia.

2.2 DTC approach of five-phase PMSM

The basic principle of DTC technique enables independent control of the stator flux and electromagnetic torque. This allows for a rapid and precise torque response in the stationary (α, β) subspace. An appropriate voltage vector is chosen from a switching table, a critical step as the selected switching state directly influences variations in the motor's torque and flux. Consequently, the optimal state is selected to maintain the torque and stator flux magnitudes within predefined hysteresis bands. DTC controls the opening and closing of the voltage source inverter switches by directly determining the control sequence that is applied to these switches [30]. The switching table for conventional DTC technique is presented in Tab. 1.

Expressed in terms of current i and flux stator Φ, the electromagnetic torque of the five-phase PMSM is given by the following equation:

$$T_e = \frac{5}{2} p\left(\Phi_\alpha i_\beta - \Phi_\beta i_\alpha\right) \tag{4}$$

Errors in the torque and flux dictate which switching states the inverter employs:

$$\begin{cases} \Delta\Phi_s = {\Phi_s}^* - \Phi_s \\ \Delta T_e = {T_e}^* - T_e \end{cases} \tag{5}$$

where

T_e^* is the reference torque,
Φ_s^* is the reference flux.

Employing the Concordia transformation, the amplitude of the flux is given by:

$$\Phi_s = \sqrt{{\Phi_\alpha}^2 + {\Phi_\beta}^2} \tag{6}$$

The angle θ_s between Φ_α and Φ_β is calculated as:

$$\theta_s = \tan^{-1}\left(\Phi_\beta / \Phi_\alpha\right) \tag{7}$$

Table 1. DTC switching table

Flux sector		1	2	3	4	5	6	7	8	9	10
Flux	Torque										
$\Delta\Phi_s$=0	ΔT_e=1	V14	V6	V7	V3	V19	V17	V25	V24	V28	V12
	ΔT_e=–1	V7	V3	V19	V17	V25	V24	V28	V12	V14	V6
	ΔT_e=0	V31	V0	V31	V0	V31	V0	V31	V0	V31	V0
$\Delta\Phi_s$=1	ΔT_e=1	V24	V28	V12	V14	V6	V7	V3	V19	V17	V25
	ΔT_e=–1	V17	V25	V24	V28	V12	V14	V6	V7	V3	V19
	ΔT_e=0	V0	V31	V0	V31	V0	V31	V0	V31	V0	V31

The standard DTC scheme for a five-phase PMSM is presented in the block diagram of Fig. 2.

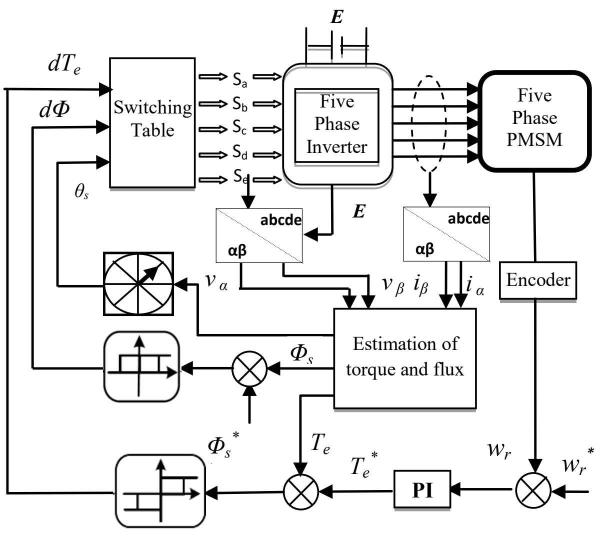

Fig. 2. Designed DTC technique of five-phase PMSM

3 Five-phase SVM technique

Conventional SVM techniques employ space vectors to overcome the mathematical complexity of deriving the angle and sector directly from the reference voltage. Instead, this calculation is simplified by first applying the Clarke transformation to the 3-phase voltages and then processing them in the stationary (α, β) subspace [31].

This paper introduces a streamlined modified SVM strategy for five-phase voltages. The approach determines suitable switching states by analyzing the extreme values (minimum and maximum) of the five phase voltages (V_a, V_b, V_c, V_d, and V_e). This modified SVM technique was chosen for its straightforward implementation and operational simplicity. Additionally, it is anticipated to achieve enhanced system performance compared to both standard Pulse Width Modulation (PWM) and traditional SVM methods. The core principle of the five-phase modified SVM applied to a two-level inverter is depicted schematically in Fig. 3. This modified five-phase SVM method follows a four-step process: identifying the minimum input voltage (V_a - V_e), finding the maximum input voltage, adding these two values together, and ultimately synthesizing the output pulses for switches S_a through S_e.

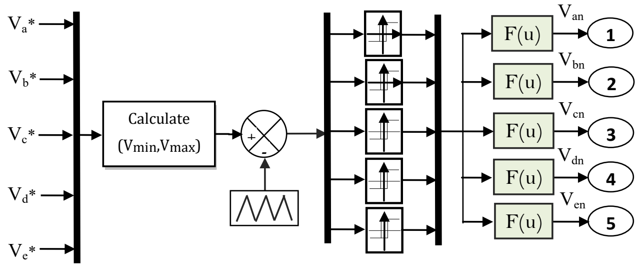

Fig. 3. Five-phase MSVM technique

4 FOSTSMA-DTC strategy based MSVM

The HOSMC approach was developed to reduce or eliminate the chattering phenomenon inherent in conventional SMCs, while preserving their essential robustness in the face of system uncertainties. Among its variants, the second-order form (exemplified by the Super-Twisting Algorithm (STA) controller) is particularly favored in nonlinear control applications due to its straightforward implementation and strong robustness [32, 33]. This algorithm differs from other SMC approaches by implementing a second-order continuous sliding mode control. Its key innovation is that it requires only knowledge of the sliding surface S, without needing to determine the sign of ($\dot{S}$). STA's combination of durability, ease of implementation, simplicity, and tunable response has driven its adoption in areas like control systems, electronics, and renewable energy [34, 35].

The STA control law given in (8) combines two elements: a component u_1 defined through its time derivative and a component u_2 expressed as a function of the sliding surface variance S.

$$u_{ST}(t) = u_1(t) + u_2(t) \tag{8}$$

$$\begin{cases} u_1 = \zeta |S|^{\gamma} \operatorname{sign}(S) \\ \dot{u}_2 = \eta . \operatorname{sign}(S) \end{cases} \tag{9}$$

Here, e represents the error, and η and ζ are positive coefficients. The value of γ is set to 0.5.

Rather than just replacing the conventional STA, the Fractional-Order STA (FOSTA) is a more powerful and flexible extension. By incorporating fractional calculus, it gains a memory effect and additional parameters that allow it to achieve faster convergence, higher tracking precision, and improved robustness. This method also significantly reduces chattering. Despite its greater computational and analytical demands, FOSTA's enhanced performance makes it a compelling choice for high-performance systems that exceed the capabilities of the traditional STA.

This controller merges the STA with fractional calculus, preserving the STA's characteristic simplicity and ease of use. Unlike the STA implementations proposed in [36], this new FOSTA design is an enhanced variant developed to achieve greater robustness and durability.

The mathematical formulation for the developed FOSTA technique is defined by the following equation:

$$\begin{cases} u = [\zeta|S|^{\gamma}\text{sign}(S) + u_1]^{\varsigma} \\ \dot{u}_1 = \eta.\text{sign}(S) \end{cases} \tag{10}$$

where $\varsigma \neq 1$.

Figure 4 illustrates the structural design employed for the FOSTA controller's implementation.

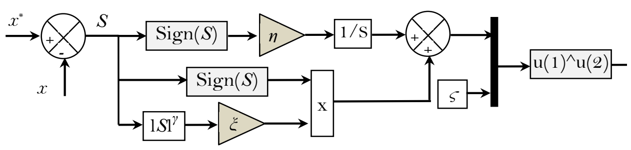

Fig. 4. The FOSTA controller

Conventional DTC schemes for multiphase PMSMs operate using hysteresis comparators and switching tables, while other implementations leverage SVM techniques with PI regulators. However, both strategies increase torque ripple, thereby diminishing system robustness [37-39].

This work develops a fractional-order super-twisting sliding mode algorithm (FOSTSMA) controller to enhance the performance and efficiency of DTC of five-phase PMSM.

The following is the selection of the sliding surfaces based on (3) and (4):

$$\begin{cases} S(w_r) = \omega_r{}^* - \omega_r \\ S(T_{em}) = T_e{}^* - T_e \\ S(\Phi_s) = \Phi_s{}^* - \Phi_s \end{cases} \tag{11}$$

Based on fractional-order super-twisting sliding mode theory, the control laws for regulating stator flux, speed, and electromagnetic torque can be formulated using the switching surfaces as their inputs.

$$\begin{cases} i_{qs}{}^* = [\zeta_1|S(\omega_r)|^{\gamma}\text{sign}(S(\omega_r)) + i_{qs}]^{\varsigma} \\ i_{qs} = \eta_1.\text{sign}(S(\omega_r)) \end{cases} \tag{12}$$

$$\begin{cases} v_{qs}{}^* = [\zeta_2|S(T_e)|^{\gamma}\text{sign}(S(T_e)) + v_{qs}]^{\varsigma} \\ \dot{v}_{qs} = \eta_2.\text{sign}(S(T_e)) \end{cases} \tag{13}$$

$$\begin{cases} v_{ds}{}^* = [\zeta_3|S(\Phi_s)|^{\gamma}\text{sign}(S(\Phi_s)) + v_{ds}]^{\varsigma} \\ \dot{v}_{ds} = \eta_3.\text{sign}(S(\Phi_s)) \end{cases} \tag{14}$$

To ensure the sliding manifolds converge to zero in finite time, the gains may be chosen according to the following criteria [36]:

$$\begin{cases} \eta_j > \dfrac{\lambda_j}{\eta_{mj}}, \quad \zeta_j{}^2 \geq \dfrac{4\lambda_j}{\eta^2{}_{mj}} \dfrac{\eta_{Mj}(\eta_j + \lambda_j)}{\eta_{mj}(\eta_j - \lambda_j)} \\ 0 < \gamma \leq 0.5; \quad j\text{=}1, 2, 3. \end{cases} \tag{15}$$

The developed FOSTSMA controllers are implemented within the DTC scheme, which utilizes MSVM for the five-phase PMSM, as shown in Fig. 5.

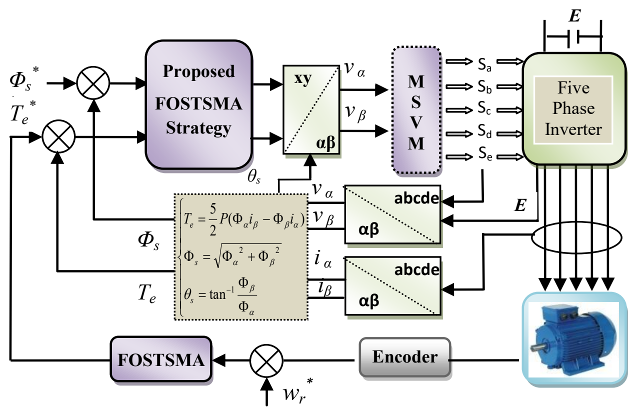

Fig. 5. Global scheme of the DTC-MSVM approach using FOSTSMA controllers for the five-phase PMSM

5 Simulation and analysis

To confirm the validity and performance of the suggested approach, simulations were conducted in MATLAB environment. The results of this new approach were then compared to those from two other methods: a conventional DTC (DTC-C) and a DTC with MSVM using a PI controller (DTC-MSVM-PI). The five-phase PMSM parameters listed in Tab. 2 [14]. The effectiveness of the proposed technique will be evaluated through a series of performance tracking and robustness tests, and its results will be compared with those from alternative methods. Numerical and graphical analysis will be used to demonstrate the designed approach's superior capability in enhancing system properties.

Table 2. Parameters of the five-phase PMSM

Parameters	Value
Nominal power P_n	1.5 kW
Stator resistance R_S	0.67 Ω
Number of pairs poles P	2
Leakage stator inductance L_l	0.00093 H
Direct stator inductance L_d	0.0085 H
Quadrature stator inductance L_q	0.0085 H
Moment of inertia J_m	0.004 kg/m^2
Frequency	50 Hz
Magnetic flux ϕ_f	0.2 Wb
DC bus voltage V_{dc}	400 V

5.1 Reference tracking and disturbance rejection

This test evaluates how the proposed DTC-MSVM-FOSTSMA strategy performs of a five-phase PMSM by tracking various speed references under the influence of T_l variation. The simulations aim to demonstrate the control's effectiveness under different operating conditions. To assess the five-phase PMSM performance, the motor's was initially operated at a constant speed of 75 rad/s with no load. The speed was then increased in a series of ramps: first to 100 rad/s at 0.2 s, then to 125 rad/s at 0.4 s. A nominal T_l=10 Nm was applied from 0.6 s to 0.8 s, after which the speed command was reversed to –25 rad/s at 1 s.

Figure 6 illustrates the rotational speed of the five-phase PMSM using three different control techniques: DTC-C, DTC-MSVM-PI, and the proposed technique DTC-MSVM-FOSTSMA. While all three methods allow the motor's mechanical speed to closely follow its reference, the response time of the suggested method is notably quicker than that of the DTC-C and DTC-MSVM-PI techniques. When the proposed technique was used, the five-phase PMSM achieved a speed response time of just 0.015 s. This represents a significant improvement of 78.57% over the DTC-MSVM-PI technique and an even greater improvement of 83.33% compared to the DTC-C technique. Additionally, with the implementation of the DTC-MSVM-FOSTSMA technique, the five-phase PMSM demonstrated a superior ability to manage speed disturbances, achieving a low rejection rate of approximately 1.6% (see Tab. 5). This marks a considerable gain in performance when compared to the 11.2% rejection rate observed with the DTC-C technique and the 5.6% rate associated with the DTC-MSVM-PI technique.

Figure 7 displays the torque T_e simulation results. The proposed technique limits torque ripple in the five-phase PMSM to 2.9 Nm. This marks a substantial improvement over conventional DTC (7.6 Nm ripple) and the DTC-MSVM-PI approach (4.3 Nm ripple), achieving ripple reductions of approximately 61.84% and 32.55%, respectively (see Tab. 5).

Figure 8 illustrates the stator flux for the five-phase PMSM across three different control strategies. In all cases, the flux maintains a constant value that closely matches the reference, even with system variations. As presented in Tab. 5, the DTC-MSVM-FOSTSMA strategy significantly reduces ripples by 0.0055 Wb, outperforming both the DTC-C Method (0.0133 Wb) and DTC-MSVM-PI techniques (0.0084 Wb).

The presence of torque and flux ripples using the proposed technique, despite their low ripples compared to other methods, is due to the chattering phenomenon known in sliding mode algorithm implementations. The observed undulations are a form of residual chattering. Although their amplitude is generally smaller and their frequency higher, but they are still present due to the reason finite switching frequency and discrete implementation.

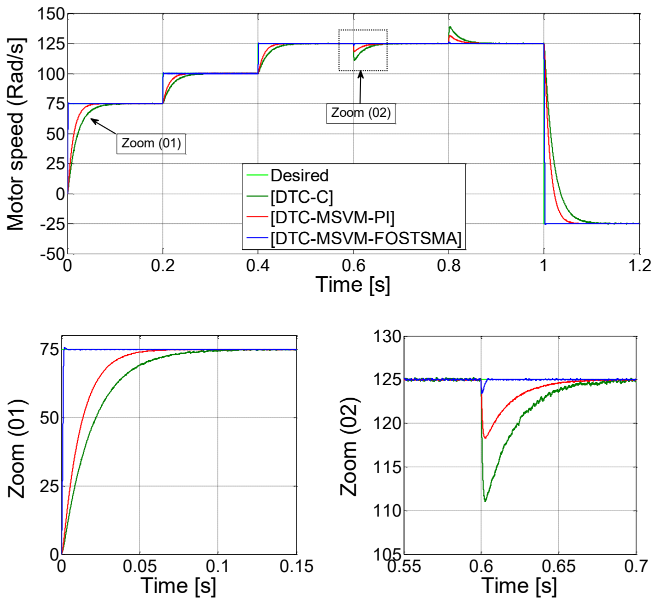

Fig. 6. Rotation speed

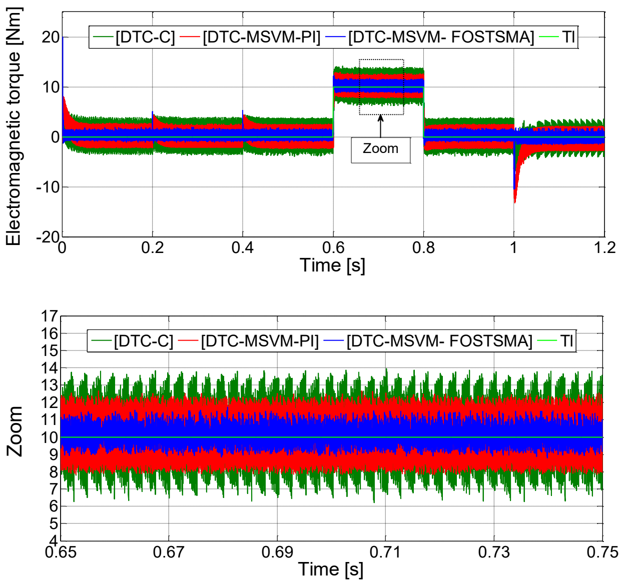

Fig. 7. Electromagnetic torque

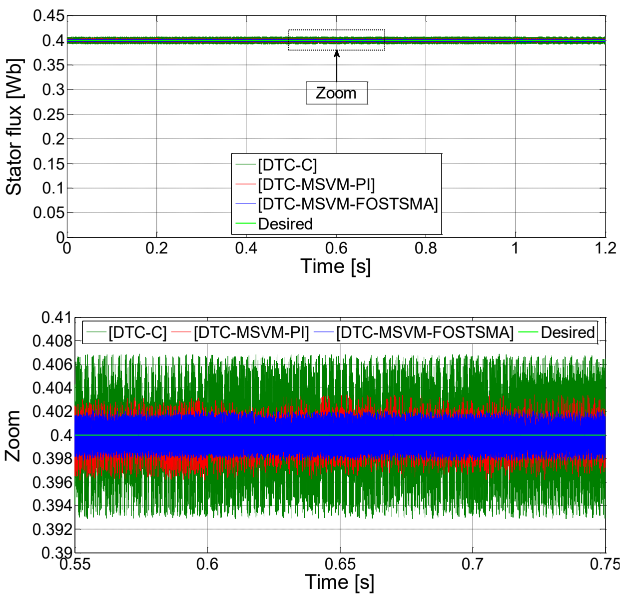

Fig. 8. Stator flux

The parameter values for the PI and FOSTSMA controllers employed in this study are listed in Tables 3 and 4.

Table 3. PI controller parameters

Controller	Coefficient	Value
Speed	K_P K_i	520 12
Stator flux	K_P K_i	200 0.1
Torque	K_P K_i	170 0.5

Table 4. FOSTSMA controller parameters

Controller	Coefficient	Value
Speed	ς ζ η	1.05 0.5 30
Stator flux	ς ζ η	1.2 0.003 12
Torque	ς ζ η	0.95 0.01 15

Table 5. Comparative analysis of the different techniques

	DTC-MSVM-FOSTSMA	DTC-MSVM-PI	DTC-C
ω_r response time (s)	0.015 s	0.07 s	0.09 s
Flux ripples (Wb)	0.3972-0.4027	0.3956-0.4040	0.3932-0.4065
Torque ripples (N.m)	8.6-11.5	7.9-12.2	6.2-13.8
ω_r dropping due to T_l application (rad/s)	123	118	111

5.2 Parameters variation tests

5.2.1 Stator resistance variations

The goal of this scenario is to evaluate the control system's robustness when faced with a sudden change in stator resistance. Specifically, the resistance is doubled (200%) at t=0.7 s, as depicted in Fig. 9. The motor's performance is tested under a constant nominal load of 10 Nm, applied between 0.6 s and 0.8 s.

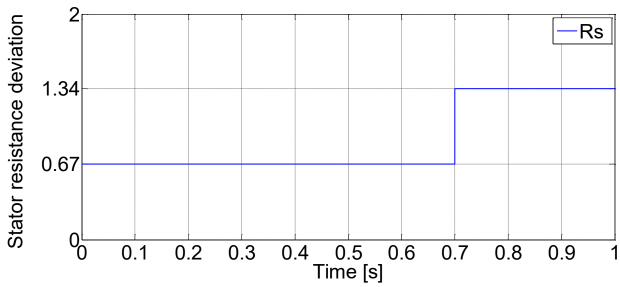

Fig. 9. Profile of the R_s deviation

During this test, the five-phase PMSM started with no load and a constant speed of 75 rad/s. The motor's speed was then increased in two separate steps. It was ramped up to 100 rad/s at the $t = 0.2$ s, followed by a second increase to 125 rad/s at $t = 0.4$ s. As shown in Fig. 10, all three techniques enabled the motor to follow its target speed. However, the proposed method was the only one that maintained accurate speed tracking when the resistance increased. Both the traditional and second methods showed a clear degradation in performance under the same conditions.

Figure 11 shows the behavior of the motor torque. At t=0.7 s, which corresponds to an increase in stator resistance, the torque oscillation and dynamics change depending on the use of each technique. When compared to other methods, the proposed DTC-MSVM-FOSTSMA technique led to a notable reduction in torque oscillations for the five-phase PMSM. The technique limited the torque ripple to a mere 3.1 Nm, a substantial enhancement over the 10.2 Nm ripple of the DTC-C technique and the 5.2 Nm of the DTC-MSVM-PI method.

Figure 12 illustrates the evolution of the stator flux. The proposed DTC-MSVM-FOSTSMA method significantly reduces flux oscillations in the five-phase PMSM. It holds the flux ripple to just 0.0061 Wb, which is a major improvement over the 0.0182 Wb ripple from the DTC-C technique and the 0.0101 Wb from the DTC-MSVM-PI method.

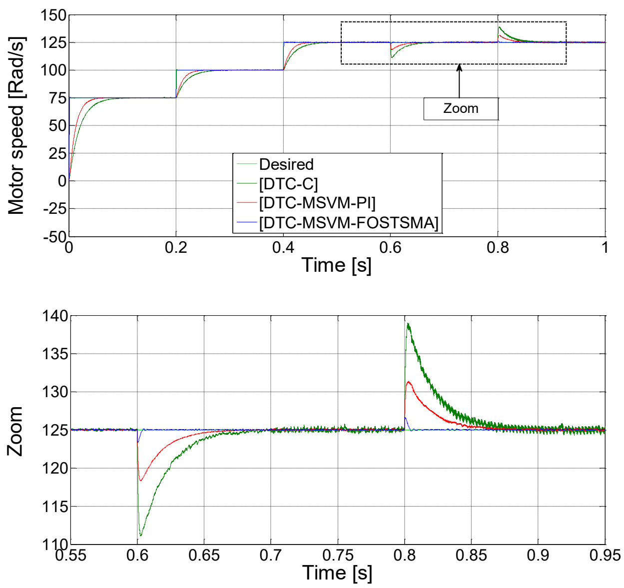

Fig. 10. Rotation speed

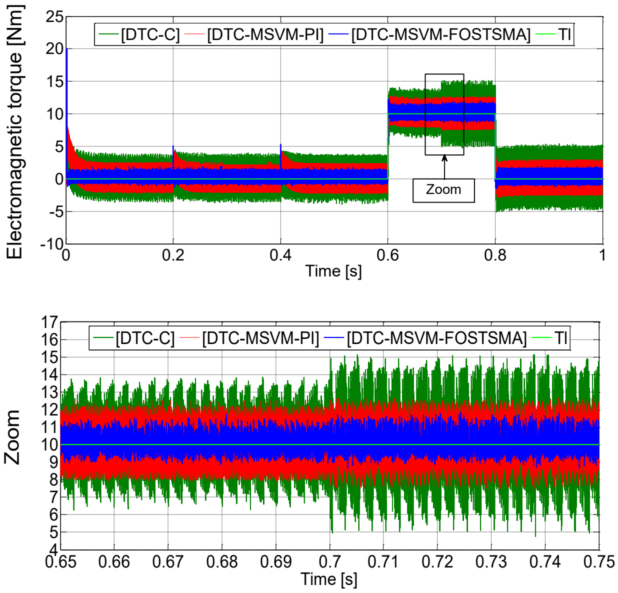

Fig. 11. Electromagnetic torque

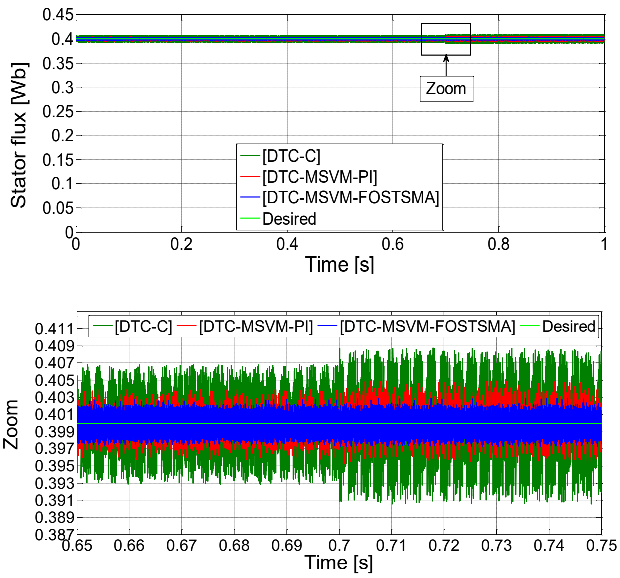

Fig. 12. Stator flux

5.2.2 Moment of inertia variation

The second robustness test evaluates the robustness of the proposed approach by increasing the moment of inertia J_m by 100%. The DTC-C and DTC-MSVM-PI method performance is more susceptible to variations in inertia parameters compared to the proposed DTC-MSVM-FOSTSMA technique for the five-phase PMSM, as depicted in Fig. 13. Additionally, unlike the smooth performance of the proposed technique for the five-phase PMSM, which tracks the reference speed without overshoot, the DTC-C and DTC-MSVM-PI method causes the speed to overshoot both at startup and during the reversal to 25 rad/s (at t=1 s).

As shown in Figs. 14 and 15, changes in inertia directly affect the torque and flux responses of a five-phase PMSM during speed changes. The proposed control scheme demonstrates superior performance, as it is less sensitive to these inertial effects compared to the DTC-C and DTC-MSVM-PI techniques.

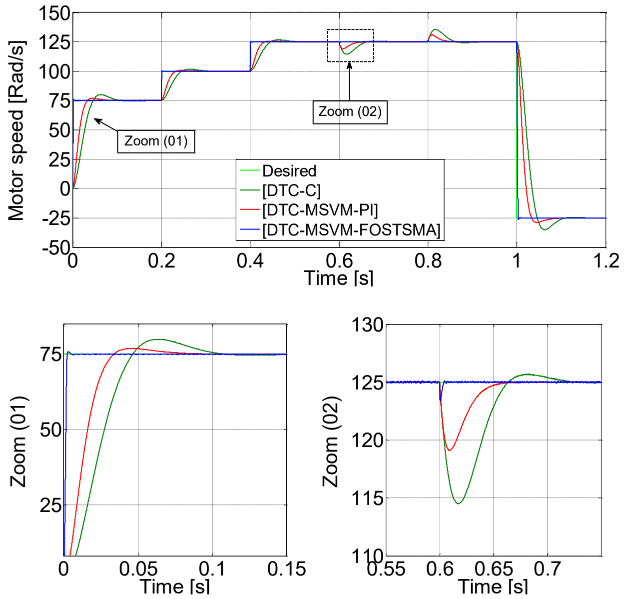

Fig. 13. Rotation speed

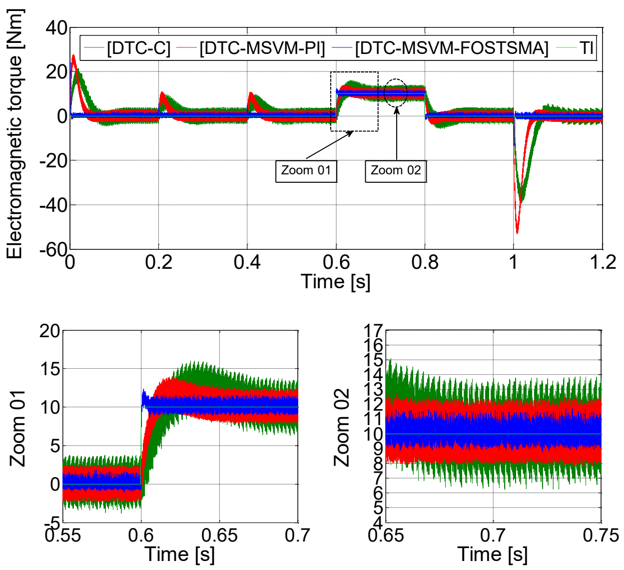

Fig. 14. Electromagnetic torque

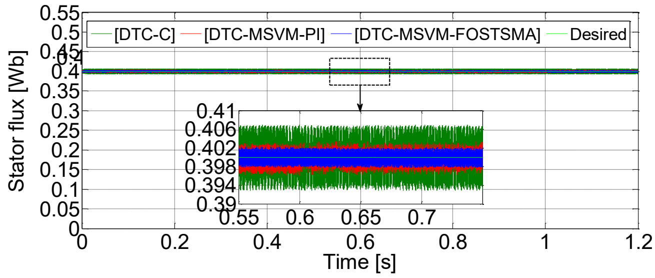

Fig. 15. Stator flux

6 Conclusion

This study introduces a nonlinear dynamic control strategy for five-phase PMSM. The approach merges a FOSTSMA with a MSVM approach, all under the framework of DTC technique. The suggested control technique was tested and evaluated in a MATLAB environment. The performance of this new approach was then directly compared to a conventional DTC and a DTC-MSVM-PI technique to demonstrate its effectiveness. The efficacy of the proposed method was assessed using several key performance metrics: reference tracking accuracy, response time, system robustness, and the minimization of fluctuations in both flux and torque.

The simulation results validated that the suggested method improves the operational efficiency of the five-phase PMSM across various conditions. Notably, it significantly boosted the motor's dynamic speed response. It achieved a reduction of 78.57% and 83.33% when compared to the DTC-MSVM-PI and DTC-C method, respectively. The suggested technique substantially lessened motor torque ripple and flux ripple. When compared to the DTC-C method, the five-phase PMSM showed a reduction in torque ripple of approximately 61.84% and a reduction in flux ripple of about 58.64%. Furthermore, when measured against the DTC-MSVM-PI approach, the torque ripple was reduced by 32.55% and the flux ripple by 34.52%. In addition, the proposed method is more robust than traditional DTC approaches, as it maintains strong performance despite changes in five-phase PMSM parameters and load disturbances.

Future research will propose extending the control strategy to include advanced controls using artificial intelligence algorithms to eliminate chattering and ensure fault-tolerant operation. Furthermore, experimental verification will be conducted to confirm the results obtained through simulation.

References

[1] M. Gholamian, O. Beik and M. Arshad, “A Review of State-of-the-Art Multiphase and Hybrid Electric Machines”, *Electronics*, vol. 13, no. 18, pp. 3636, 2024. doi:10.3390/electronics13183636.

[2] Z. Frank, J. Laksar and K. Hruska, “Overloadability improvement of electric motorcycle eDrive by using a five-phase PMSM”, *Electrical Engineering*, vol. 107, pp. 14191-14203, 2025. doi: 10.1007/s00202-025-03255-9.

[3] M. Wang, P. Li, Y. Li, W. Jia and Y. Shen, “Analysis of a Novel Consequent-Pole Dual-Stator Linear Permanent Magnet Vernier Machine Employing Mover Slot PM”, *IEEJ Trans*, vol. 20, no. 1, pp. 101-113, 2025. doi:10.1002/tee.24174.

[4] A. Singh and A. Khosla “A survey and analysis of multiphase electric propulsion motors and associated controllers for driving underwater platforms”, *Propulsion and Power Research*, vol. 14, no. 2, pp. 304-321, 2025. doi:10.1016/j.jppr.2025.06.001.

[5] A. Ajmi, S. krim, A. Hosseyni, M. Mansouri and M. F. Mimouni, “Robust Variable Structure Control Approach of Two Series-Connected Five-Phase PMSMs Under Healthy and Faulty Operation Modes”, *IEEE Access*, vol. 11, pp. 96401-96422, 2023. doi: 10.1109/ACCESS.2023.3311029.

[6] H. Liu, W. Niu and Y. Guo, “Direct torque control for PMSM based on the RBFNN surrogate model of electromagnetic torque and stator flux linkage”, *Control Engineering Practice*, vol. 148, pp. 105943, 2024. doi: 10.1016/j.conengprac.2024.105943

[7] T. L. Le and M. F. Hsieh, “An enhanced direct torque control strategy with composite controller for permanent magnet synchronous motor” , *Asian Journal of Control*, vol. 26, no. 4, pp. 1683-1702, July. 2024. doi:10.1002/asjc.3306

[8] M. G. Simon and D. Fodor, “Comparative Analysis of Field Oriented Control and Direct Torque Control Through Simulation in MATLAB Simulink for an Automotive Drive Motor”, *Engineering Proceedings*, vol. 79, no. 1, pp. 33, 2024. doi: 10.3390/engproc2024079033

[9] S. Mondal, P. Roy, A. Banerjee and U. Mondal, “A CKF-based sensor-less FOC integrated with gh-SVPWM for PMSM drives”, *Electrical Engineering*, vol. 106, pp. 3461-3473, 2024. doi: 10.1007/s00202-023-02169-8

[10] R. Dermouche, A. Talaoubrid, M. Fazilat, N. Zioui and M.Tadjine, “A quantum direct torque control method for permanent magnet synchronous machines”, *Computers and Electrical Engineering*, vol. 122, pp. 109994, 2025. doi: 10.1016/j.compeleceng.2024.109994

[11] R. Araria, A. Berkani, K. Negadi, F. Marignetti and M. Boudiaf, “Performance analysis of DC-DC converter and DTC based fuzzy logic control for power management in electric vehicle application”, *Journal European des Systèmes Automatisés*, vol. 53, no. 1, pp. 1-9, 2020. doi: 10.18280/jesa.530101

[12] K. Kakouche, A. Oubelaid, S. Mezani, D. Rekioua and T. Rekioua, “Different Control Techniques of Permanent Magnet Synchronous Motor with Fuzzy Logic for Electric Vehicles: Analysis, Modelling, and Comparison”, *Energies*, vol. 16, no. 7, pp. 3116, 2023. doi: 10.3390/en16073116

[13] A. Bıçak and A. Gelen, “Sensorless direct torque control based on seven-level torque hysteresis controller for five-phase IPMSM using a sliding-mode observer”, *Engineering Science and Technology, an International Journal*, vol. 24, no. 5, pp. 1134-1143, 2021. doi:10.1016/j.jestch.2021.02.004

[14] B. Cao, B. M. Grainger, X. Wang, Y. Zou, G. F. Reed, and Z. H. Mao, “Direct torque model predictive control of a five-phase permanent magnet synchronous motor”, *IEEE Trans. Power Electron*, vol. 36, no. 2, pp. 2346-2360, 2021. doi: 10.1109/TPEL.2020.3011312

[15] M. L. De Klerk and A. K. Saha, “Performance Analysis of DTC-SVM in a Complete Traction Motor Control Mechanism for a Battery Electric Vehicle”, *Heliyon*, vol. 8, no. 4, pp. 09265, 2022. doi: 10.1016/j.heliyon.2022.e09265

[16] S. Manala and J. Seshadrinath, “Robust Model-Based Interturn Fault Detection in DTC-SVM PMSM Drive”, *IEEE Sensors Journal*, vol. 25, no. 20, pp. 39027-39036, 2025. doi: 10.1109/JSEN.2025.3609012

[17] S. A. A. Tarusan, A. Jidin, and M. L. M. Jamil, “The optimization of torque ripple reduction by using DTC-multilevel inverter”, *ISA Transactions*, vol. 121, pp. 365-379, 2022. doi: 10.1016/j.isatra.2021.04.005

[18] A. Oubelaid, N. Taib, S. Nikolovski, T. E. A. Alharbi, T. Rekioua, A. Flah and S. S. M. Ghoneim, “Intelligent Speed Control and Performance Investigation of a Vector Controlled Electric Vehicle Considering Driving Cycles”, *Electronics*, vol. 11, no. 13, pp. 1925, 2022. doi: 10.3390/electronics11131925

[19] H. Mesloub, M. T. Benchouia, R. Boumaaraf, A. Goléa, N. Goléa and M. Becherif, “Design and implementation of DTC based on AFLC and PSO of a PMSM”, *Mathematics and Computers in Simulation*, vol. 167, pp. 340-355, 2020. doi: 10.1016/j.matcom.2018.04.010

[20] Y. Tian, Y. Zhang, X. Xiao and T. Yildirim, “Weighting factors design in model predictive direct torque control based on cascaded neural network”, *Asian Journal of Control*, vol. 26, no. 3, pp. 1323-1338, 2024. doi: 10.1002/asjc.3262

[21] M. Sellah, A. Kouzou and M. M. Rezaoui, “Investigation of SVPWM based sliding mode control application on dual-star induction motor and dual open-end winding induction motor”, *Periodica Polytechnica Electrical Engineering and Computer Science*, vol. 66, no. 1, pp. 80-98, 2022. doi:10.3311/ppee.17910

[22] Z. Zhang, Z. Chen, N. Li, K. Chen, N. C. Cheung, J. Pan, “A dynamic convergence second-order sliding mode control structure for PMSM with an observer based on a novel sliding mode reaching law”, Control Engineering Practice, vol. 164, pp. 106504, 2025. doi: 10.1016/j.conengprac.2025.106504

[23] A. Kareem, V. P. Basheer and V. Kumara, “A Second-Order Sliding Mode Control Scheme With Fuzzy Logic-Based Online Sliding Surface Adjustment for Buck Converters”, *IEEE Access*, vol. 13, pp. 48792-48801, March. 2025. doi:10.1109/ACCESS.2025.3551127

[24] M. A. Mossa, H. Echeikh , N. ElOuanjli and H. H. Alhelou, “Enhanced Second-Order Sliding Mode Control Technique for a Five-Phase Induction Motor”, *International Transactions on Electrical Energy Systems*, vol. 1, pp. 1-19, 2022. doi: 10.1155/2022/8215525

[25] L. Hu, F. Xiao and Z. Xin, “Research on voltage regulation ability of four-level nested clamp converter based on virtual space vector modulation, ”, *IET Power Electronics*, vol. 16, no.7, pp. 1091-1102, 2023, doi:10.1049/pel2.12451.

[26] H. Benbouhenni, N. Bizon, M. Yessef, Z. M. S. Elbarbary, I. Colak, M. M. Alammar and B. Bossoufi, “Enhancing the power quality of dual rotor wind turbines using improved fuzzy space vector modulation and super twisting sliding techniques”,*Scientific Reports*, vol. 15, pp. 7290, 2025. doi:10.1038/s41598-025-90914-3.

[27] Z. Li, J. Wang, S. Feng, Y. Zhu and H. Sun, “Enhanced Low-Speed Characteristics With Constant Switching Torque-Controller-Based DTC Technique of Five-Phase Induction Motor Drive With FOPI Control”, *IEEE Transactions on Industrial Electronics*, vol. 70, no. 11, pp. 10789-10799, 2023. doi:10.1109/TIE.2022.3227275

[28] Y. Zahraoui, F. M. Zaihidee, M. Kermadi, S. Mekhilef, I. Alhamrouni, M. Seyedmahmoudian and A. Stojcevski, “Optimal tuning of fractional order sliding mode controller for PMSM speed using neural network with reinforcement learning”, *Energies*, vol.16, no. 11, pp. 4353, 2023. doi:10.3390/en16114353

[29] H. Zhou, C. Zhou, W. Tao, J. Zhu, J. Wang and G. Liu, "Virtual-Stator-Flux-Based Direct Torque Control of Five-Phase Fault-Tolerant Permanent-Magnet Motor With Open-Circuit Fault", *IEEE Transactions on Power Electronics*, vol. 35, no. 5, pp. 5007-5017, May. 2020. doi:10.1109/TPEL.2019.2942397

[30] G. Li, J. Hu, Y. Li and J. Zhu, "An Improved Model Predictive Direct Torque Control Strategy for Reducing Harmonic Currents and Torque Ripples of Five-Phase Permanent Magnet Synchronous Motors", *IEEE Transactions on Industrial Electronics*, vol. 66, no. 8, pp. 5820-5829, August. 2019. doi:10.1109/TIE.2018.2870359

[31] H. Benbouhenni, N. Bizon and I. Colak, "A Brief Review of Space Vector Modulation (SVM) Methods and a New SVM Technique Based on the Minimum and Maximum of the Three-Phase Voltages", *Iranian Journal of Electrical and Electronic Engineering*, vol. 3, pp. 2358, 2022. doi:10.22068/IJEEE.18.3.2358

[32] S. Liu, X. Liu, S. Jiang, Z. Zhao, N. Wang, X. Liang, M. Zhang and L. Wang, "Application of an Improved STSMC Method to the Bidirectional DC–DC Converter in Photovoltaic DC Microgrid", *Energies*, vol. 15, no. 5, pp. 1636, 2022. doi:10.3390/en15051636

[33] I. González-Hernández, S. Salazar, R. Lozano and S. Ramírez-Ayala, "Real-Time Improvement of a Trajectory-Tracking Control Based on Super-Twisting Algorithm for a Quadrotor Aircraft", *Drones*, vol. 6, no. 2, pp. 36, 2022. doi:10.3390/drones6020036

[34] Y. Wang and C. Ji, "A Passive Fault Tolerance Strategy for Super-Twisting Algorithm-Based Sliding Mode Control with Barrier Function for Quadrotor UAVs", *IEEE Access*, vol. 13, pp. 115321-115330, July. 2025. doi:10.1109/ACCESS.2025.3585408

[35] K. Lochan, L. Seneviratne and I. Hussain, "Adaptive Global Super-Twisting Sliding Mode Control for Trajectory Tracking of Two-Link Flexible Manipulators", *IEEE Access*, vol. 13, pp. 61876-61889, April. 2025. doi:10.1109/ACCESS.2025.3557202

[36] I. Sami, U. Shafaat, S. Ul-Amin, A. Al-Durra, A. Nasim and R. JongSuk, "Convergence enhancement of super-twisting sliding mode control using artificial neural network for DFIG-based wind energy conversion systems", *IEEE Access*, vol. 10, pp. 97625–97641, 2022. doi:10.1109/ACCESS.2022.3205632

[37] F. Mehedi, H. Benbouhenni, L. Nezli and D. Boudana, "Feedforward Neural Network-DTC of Multi-phase Permanent Magnet Synchronous Motor Using Five-Phase Neural Space Vector Pulse Width Modulation Strategy", *Journal Européen des Systèmes Automatisé*, vol. 54, no. 2, pp. 345-354, 2021. doi:10.18280/jesa.540217

[38] Z. Liu, H. Zhou, Z. Zhou and G. Liu, "Torque dynamic performance enhancement of five-phase permanent magnet synchronous motor with open-circuit fault", *IET Electric Power Applications*, vol. 18, no. 11, pp. 1530-1539, 2024. doi:10.1049/elp2.12513

[39] A. Mastanaiah, T. Ramesh, S. V. K. Naresh, P. K. Bonthagorla, "Deep Reinforcement Learning Agent Based Speed Controller for DTC-SVM of PMSM Drive", *IET Power Electronics*, vol. 18, no. 1, pp. 1-13, 2025. doi: 10.1049/pel2.70130

Received 14 September 2025